Technical Review

No. 4 · 1987

Windows to FFT Analysis (Part II)
Acoustic Calibrator for Intensity Measurement Systems

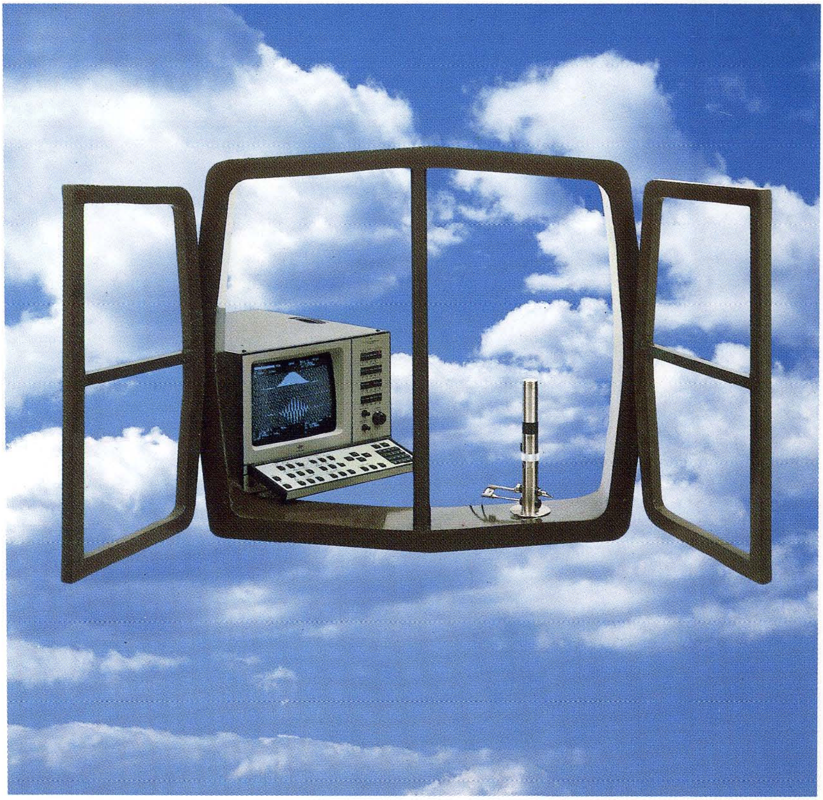

Brüel & Kjær

Previously issued numbers of Brüel & Kjær Technical Review

(Continued on cover page 3)

Technical Review

No. 4 · 1987

Contents

'se of Weighting Functions in 'FT/FFT Analysis (Part II)

Svend Gade and
ɜnrik Herlufsen

bstract

rt II of the article "Use of Weighting Functions in DFT/FFT analysis" ntains the following Appendices referred to in Part I of the article

Analogy between filter analysis and DFT/FFT analysis,
Windows and figures of merit,
Effective Weighting of overlapped spectral averaging
Experimental Determination of the BT product for FFT-analysis using different weighting functions and overlap,
Examples of User Defined Windows,
Picket Fence Effect

ɔmmaire

La deuxième partie de cet article, "Application des fonctions de pondé-tion en analyse DFT/FFT", contient les appendices auxquels fait réfé-nce la première partie.

Analogie entre l'analyse par filtres et l'analyse DFT/FFT.
Caractéristiques des fenêtres.
Pondération effective des moyennes de spectres avec recouvrement.
Détermination expérimentale du produit BT en analyse FFT, avec différentes fonctions de pondération et recouvrements.
Exemples de fenêtres définies par l'utilisateur.
Effet de barrière.

usammenfassung

Der zweite Teil des Artikels „Anwendung von Bewertungsfunktionen in ·r DFT/FFT-Analyse" enthält folgende Anhänge, auf die im ersten Teil ɜzug genommen wird:

Analogie zwischen Filter-Analyse und DFT/FFT-Analyse

B: Fenster und mathematische Beschreibung
C: Effektive Bewertung bei spekraler Mittelung mit Überlappen
D: Experimentelle Bestimmung des BT-Produkts bei der FFT-Anal
se mit verschiedenen Bewertungsfunktionen und Überlappunge
E: Beispiele für anwenderdefinierte Fenster
F: Lattenzauneffekt

Appendix A

Analogy between filter analysis and FFT/DFT analysis

In the time domain a linear filter is described by its impulse respon function $h(t)$, which is the response due to an infinitely short and inf nitely high unit impulse (so-called Dirac Delta function $\delta(t)$, see Ref. [1]

By considering any input signal $x(t)$ to the filter as a sum of weighte and time shifted delta functions i.e.

$$x(t) = \int_{-\infty}^{\infty} x(\tau)\,\delta(t-\tau)\,d\tau \qquad \text{(A.}$$

we find, under assumptions of linearity, that the output of the filter is

$$y(t) = \int_{-\infty}^{\infty} x(\tau)\,h(t-\tau)\,d\tau \qquad \text{(A.}$$

or since $h(t) = 0$ for $t < 0$, that

$$y(t) = \int_{-\infty}^{t} x(\tau)\,h(t-\tau)\,d\tau \qquad \text{(A.}$$

The output of a filter at a given point in time t_o is thus determined by th input time history up to time t_o weighted by the impulse response functio inverted with respect to time and shifted to t_o i.e. $h(t_o - t)$. This is illus trated in Fig. A.1 for a simple lowpass filter with an exponential decayin impulse response function. The output at time t_o, $y(t_o)$ is the integral (c the area) of the curve in Fig. A.1 d). Mathematically the calculation in eq

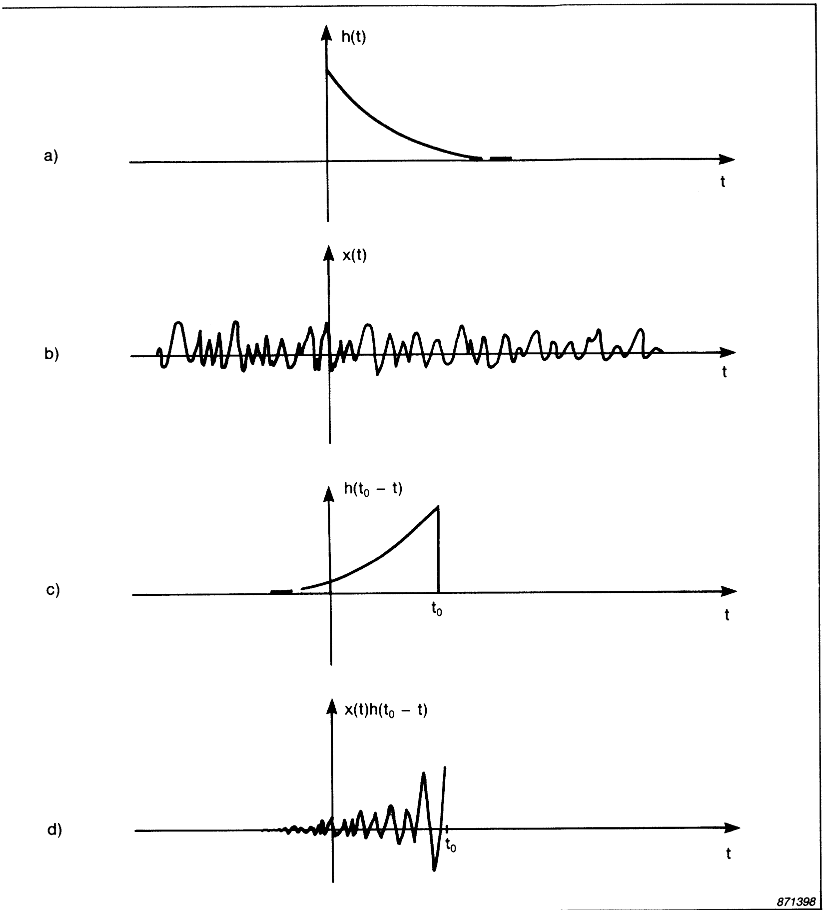

ig. A.1. a) impulse response of a simple lowpass filter h(t),
input signal to be analysed x(t),
impulse response inverted and shifted $h(t_0 - t)$,
) weighted input signal to be integrated to give output at time t_0, $y(t_0)$

\.3) is called convolution of $x(t)$ with $h(t)$ (denoted by $x(t) \star h(t)$).
Let us now have a look at the FFT/DFT calculation. To simplify the otation the integral formulation will be used instead of the discrete. The onsequence of the discrete form and finite calculation time will be disussed later. Each Fourier spectrum is a transform of the input signal $x(t)$

applied with a proper weighting function $w(t)$. The transform is based (a time record of length T.

$$Y(f) = \int_{-\infty}^{\infty} x(\tau) w(\tau) e^{-j2\pi f\tau} d\tau = \int_{0}^{T} x(\tau) w(\tau) e^{-j2\pi f\tau} d\tau \qquad \text{(A.}$$

$Y(f)$ is the output of the transform at frequency f and at time T (neglec ing for the time being the delay due to the calculation time T_{cal}). Conside ing this output at a certain frequency f_0 as a function of time $Y(f_0,$ or just $Y(t)$, we have

$$Y(t) = \int_{t-T}^{t} x(\tau)\, w\big(\tau-(t-T)\big) e^{-j2\pi f_0\left(\tau-(t-T)\right)} d\tau \qquad \text{(A.}$$

Rewriting this using

$$w_h(t) = w(-t+T) \qquad \text{(A.}$$

we get

$$Y(t) = \int_{t-T}^{t} x(\tau)\, w_h\big(-\tau+(t-T)+T\big) e^{j2\pi f_0\left(-\tau+(t-T)\right)} d\tau$$

or

$$Y(t) = \int_{t-T}^{t} x(\tau)\, w_h(t-\tau) e^{j2\pi f_0(t-\tau-T)} d\tau \qquad \text{(A.}$$

This is exactly the same equation as for a filter (eqn. A.3) and we ca define an equivalent (complex) impulse response function $h_{\text{FT}}(t)$ for tl Fourier Transform (FT) at frequency f_0 by

$$h_{FT}(t) = w_h(t)\, e^{j2\pi f_0(t-T)} \qquad \text{for} \qquad 0 \leqslant t < T \qquad \text{(A.}$$

$$h_{FT}(t) = 0 \qquad \text{elsewhere}$$

and (A.7) becomes

$$Y(t) = \int_{t-T}^{t} x(\tau)\, h_{FT}(t-\tau)\, d\tau \qquad \text{(A.}$$

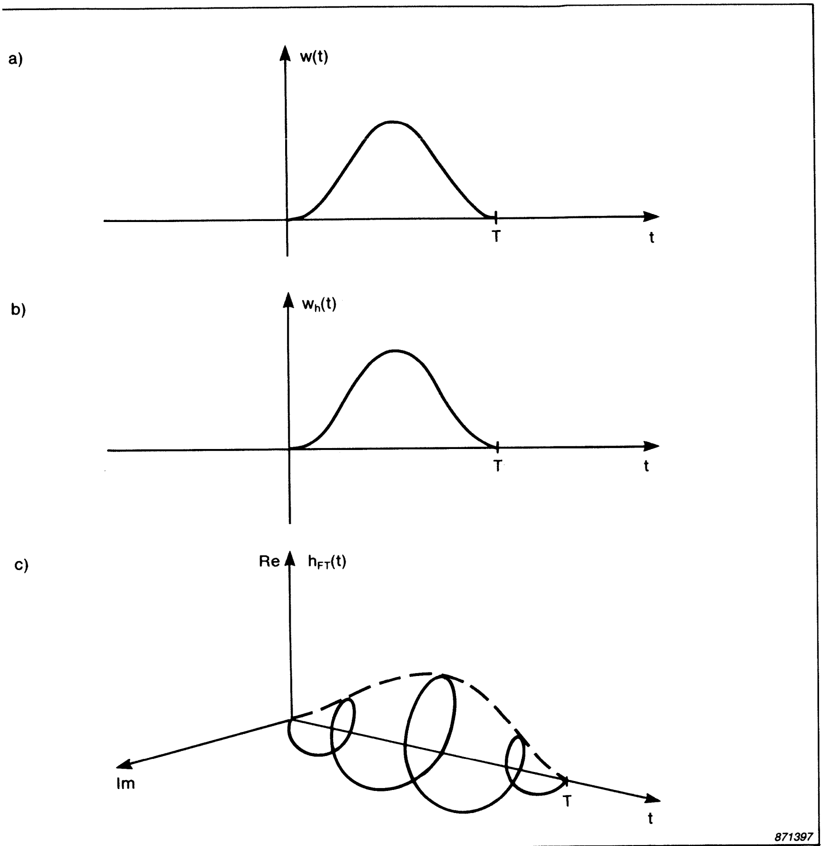

g. A.2. *a) Hanning Weighting function w(t),*
$w_h(t) = w(-t+T)$ for the Hanning Weighting,
complex impulse response function for filter/line at $f_0 = 4\,\Delta f$ with Hanning Weighting

This proves the analogy between the Finite Fourier Transform eqn. .9) and the filtering analysis eqn. (A.3). The impulse response $h_{FT}(t)$ is ›mplex and of finite length T and is determined by the weighting func- ɔn $w(t)$ (equations (A.8) and (A.6)). Fig. A.2 shows an example of a eighting function and one of the corresponding complex impulse re- ›onse functions.

Notice that for the commonly used weighting functions like Hanning, ectangular, Kaiser-Bessel and Flat Top, $w(t) = w_h(t)$ since they are symmetrical around $t = T/2$ (see also Appendix B eqn. (B.1) and table B.

So far we have used an integral formulation of the Fourier Transfor In practical calculations we will of course work with

a) sampled versions of the time signals and their spectra

b) finite calculation time T_{cal} of the transform

The transform which is discrete in both time and frequency domain called the Discrete Fourier Transform (DFT). The Fast Fourier Trar form (FFT) is a fast calculation of the DFT based on a certain algorith

re a): The time signals are sampled at time intervals $\Delta t = 1/f_s$, where f_s the sampling frequency, and the transform will be of N sampl which means that $T = N \cdot \Delta t$. The spectrum is computed at d crete frequencies $f_0 = k\,\Delta f = k\,1/T$, where k is an integer a $0 \leqslant k < N/2$. The transform is thus in its proper form written as

$$Y(k) = 1/N \sum_{n=0}^{N-1} x(n)\, w(n)\, e^{-j2\pi kn/N} \qquad \text{(A.1}$$

$x(n)$ is the n'th time sample in the record, $w(n)$ is the n'th tir sample of the weighting function and $Y(k)$ is the spectral value frequency $k\,\Delta f$. The factor $1/N$ is just a scaling factor irrelevant f the discussion here.

re b): Since we have a finite calculation time T_{cal} which in most situatio is much larger than the sample interval Δt we will not get a contin ous output as with an analog filter or a sample per sample outp every Δt as with a real time digital filter.

Every FFT represents a sample of the Fourier Transform filters (eq (A.8) and (A.9)), but the relatively long T_{cal} makes the analysis appe blockwise rather than continuous. In many applications, analysis of tra sients for instance, it is preferable to look at it as a transform of a da block with various trigger possibilities. This approach will be dealt wi later.

In a situation where $T_{cal} \leqslant \Delta t$ (analysis of very low frequencies or anal sis with very high zoom factors or much faster calculations than availab today) the FFT will be indistinguishable from a bank of real-time digit FIR (finite impulse response) filters with (complex) impulse respon functions as given in eqn. (A.8). The FFT is here assumed to work contin ously i.e. with free run triggering, as a digital filter.

Since the filtering or FFT is only part of the analysis we will now look the detector/averager.

The purpose of the detector in a filter analyzer is to measure the power ıean square) of the output signal of the filter $y(t)$, by time averaging of e squared signal $y^2(t)$. The averaging can be linear

$$ = \frac{1}{T_a} \int_{T_a} y^2(\tau)\, d\tau \qquad \text{(A.11)}$$

exponential

$$(t) = \frac{1}{\tau_0} \int_{-\infty}^{t} y^2(\tau)\, e^{(\tau - t)/\tau_0}\, d\tau \qquad \text{(A.12)}$$

hich is a continuous running average. The bar $\overline{}$ indicates average val- ›s. For a complete discussion of this subject see Ref. [1].

The averaging in the FFT analyzer is the corresponding summation of ıe squared amplitudes $|Y(i)|^2$ of the output samples $Y(i)$, where i is the me or number index. Assuming a transform every T_{cal} we will have the :h sample at time $t = t_i = i\,T_{cal}$.

This gives for linear averaging

$$\overline{|Y|^2} = \frac{1}{N} \sum_{i=1}^{N} |Y(i)|^2 \qquad \textit{(see Footnote page 35)} \qquad \text{(A.13)}$$

ıd for exponential averaging

$$\overline{|Y(i)|^2} = \frac{1}{N/2} \left(|Y(i)|^2 + (N/2 - 1)\, \overline{|Y(i-1)|^2} \right) \qquad \text{(A.14)}$$

hich is a discrete and recursive form of the analog version eqn. (A.12).

Notice that T_{cal} thus includes calculation of FFT as well as the ʋeraging.

It could now be argued that in order to get a real-time analysis in the ›nse that all input time samples are equally weighted in the averaging rocess we need to fulfil the requirement.

$$T_{cal} \leqq \Delta t \qquad \text{(A.15)}$$

s for real-time recursive digital filtering.

The weighting of the input samples in each power (mean square) calcu- ıtion $|Y(i)|^2$ is given by $|h_{FT}(t)|^2 = w_h^2(t)$, and $w_h(t) = w(t)$ for the ʼeighting functions considered here as mentioned earlier.

In linear averaging this will result in an effective weighting functic $w_{\text{eff}}(t)$ on the time data given by

$$w^2_{\text{eff}}(t) = \frac{1}{N}\sum_{i=1}^{N} w^2\left(t - iT_{\text{cal}}\right) \qquad \text{(A.1}$$

It turns out that if Hanning Weighting is used $w^2_{\text{eff}}(t)$ is uniform (flat) $T_{\text{cal}} = T/3,\ T/4,\ T/5, \ldots$, i.e. if 66 2/3 % overlap, 75% overlap, ... can be pe formed. This is shown and discussed in **Appendix C**. "True" real-tir analysis can thus be performed with Hanning Weighting if

$$T_{\text{cal}} \leqq T/3 \qquad \text{(A.1}$$

is fulfilled.

If Rectangular weighting is used no overlap would be required. This however as discussed in the article, in general a poor choice of weightir function for continuous signals.

As an example, the B & K Analyzer Type 2032 has a $T_{\text{cal}} \approx$ 50 ms i single channel mode with Hanning weighting. This gives the possibility ("true" real-time analysis (with either 66 2/3% or 75% overlap) with 3,2 kHz frequency span setting (i.e. Δf = 4 Hz, T = 250 ms).

After having discussed the analogy between filter and FFT analysis i the time domain and its limitations with respect to real-time operation w will now consider the analogy in the frequency domain.

The relation between input and output in the frequency domain for filter is

$$Y(f) = H(f) \cdot X(f) \qquad \text{(A.1}$$

where $X(f)$ and $Y(f)$ are the spectra of the input and output signals re spectively and $H(f)$ is the frequency response of the filter. This is a conse quence of eqn. (A.3) and the convolution theorem for the Fourier Trans form (Refs. [1,7,8]). $H(f)$ is the Fourier Transform of $h(t)$

$$H(f) = \mathcal{F}\{h(t)\} \qquad \text{(A.1}$$

and is called the (complex) filter characteristic, containing both amplitud and phase information.

From eqn. (A.8) we thus find that the filter characteristic for the FFT a frequency f_0 is given by

$$_{FT}(f) = \mathscr{F}\ \{w(t)\,e^{j2\pi f_o(t-T)}\} \tag{A.20}$$

ıce $w_h(t) = w(t)$ for the weighting functions considered here. Defining

$$\{w(t)\} = W(f) \tag{A.21}$$

ɜ have that

$$_{FT}(f) = \mathscr{F}\ \{w(t)e^{j2\pi f_o(t-T)}\} = W(f-f_o) \tag{A.22}$$

The filter characteristic for the filter/line at frequency f_0 is thus the Fou- ɜr Transform of the weighting function shifted to the relevant frequency . The FFT can thus be considered as a bank of parallel, identical con- ant bandwidth filters with the amplitude characteristic $|W(f-f_0)|$ i.e. $W(f)|$ centered at the frequency f_0. This is the basis for the plots of the ter amplitude characteristics for the different weighting functions 'ig. 6, 8, 11 and 15) in Part I of this article.

For analog filters the characteristics are always complex conjugate sym- etric about $f = 0$ i.e. $H(-f) = H^\star(f)$. This is not true for $W(f-f_0)$, here $f_0 \neq 0$, and the FFT output $Y(i)$, for $f_0 \neq 0$, is in general complex. The phase characteristic of the FFT filters is given by the phase of $'(f)$, $\angle W(f)$. For the weighting functions considered here which are mmetric about $t = T/2$ the phase is given by the time shift of $T/2$ as

$$W(f) = -2\pi f\,T/2 = -\pi f T = -\pi\, f/\Delta f \tag{A.23}$$

$$W(f-f_o) = -\pi\,(f-f_o)/\Delta f \tag{A.24}$$

The phase characteristic is linear with a shift of $-\pi$ for every Δf (filter/ ne spacing) see Fig. A.5 b). (A linear phase characteristic is often a main lvantage in application of FIR filters).

As already mentioned another approach for the formulation of the FFT very often used. This approach is based on the blockwise analysis and ıat the FFT line spectrum is considered as the Fourier Series of a periodic gnal with the data block (record) being one period. The derivation of the FT from the Integral Fourier Transform is given by the following steps: time sampling, b) time multiplication – frequency convolution, c) fre- ıency sampling. This is dealt with in detail in Refs. [4 and 7].

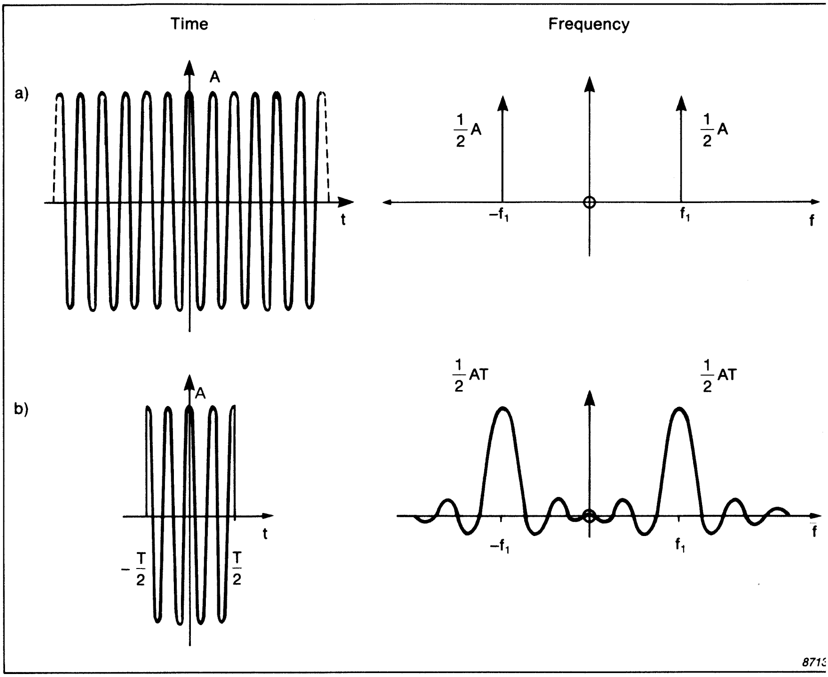

Fig. A.3. Frequency spectrum of a) a sinusoidal time signal and b) the tone burst produced by truncating the time signal in a)

Let us here take an example and see the differences and similarities of the two formulations. The signal to be analyzed is the cosine, $x(t) = A \cdot \cos(2\pi f_1 t)$ with a Fourier Spectrum as shown in Fig. A.3.a

Truncation of the signal by multiplication with Rectangular weightir of length T, produces the tone burst shown in Fig. A.3.b). The effect of this multiplication is a convolution in the frequency domain of the spec trum in Fig. A.3.a) with the spectrum of the Rectangular window $W(f) = T\,\frac{\sin(\pi f T)}{\pi f T}$ resulting in the spectrum shown in Fig. A.3.b). Th convolution is written as

$$X(f) \star W(f) = \int_{-\infty}^{\infty} X(f') \cdot W(f-f')\,df' \qquad \text{(A.2}$$

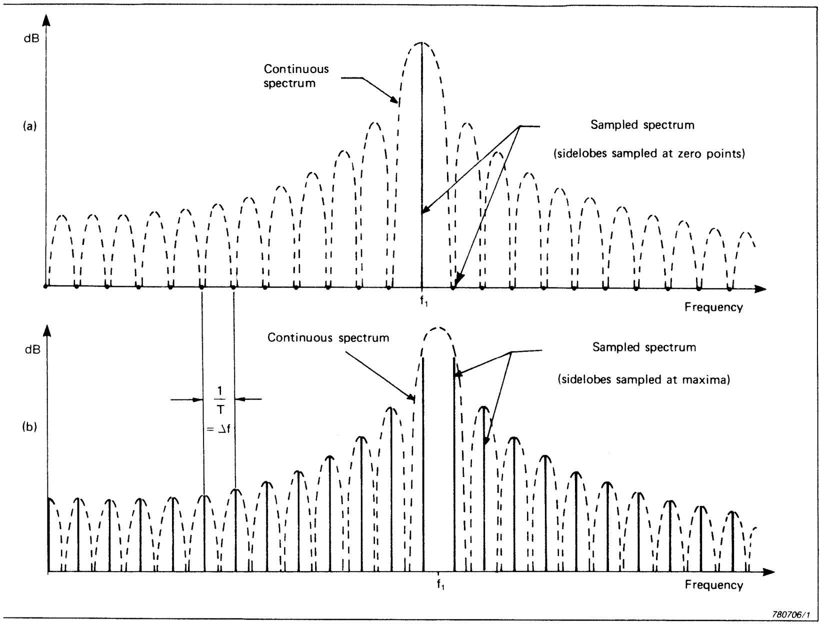

g. A.4. Frequency sampling of the continuous spectrum of the time limited sinusoid. ımber of periods within the time window (record length) is a) integer (12) half-integer ($12^1/_2$)

ıich can be interpreted as a swept filter analysis where $W(f_0 - f)$ is the ter characteristic.

The continuous spectrum is calculated i.e. sampled at the discrete fre- ıencies $f = k\,\Delta f = k\ ^1/_T$. Depending upon the frequency f_1 we will get dif- rent results as exemplified in Fig. A.4. In Fig. A.4.a) f_1 coincides with ıe of the samples, here $f_1 = 12\ \Delta f$ (corresponding to 12 periods in the cord length T), and we get only one line with the correct amplitude in the ?T spectrum. In Fig. A.4.b) however f_1 is in between two samples, here $= 12^1/_2\ \Delta f$ (corresponding to $12^1/_2$ periods in the record length T) and all e side lobes will appear in the analysis and the maximum amplitude is o low. This is also referred to as leakage.

Returning to the filter analogy let us consider a bank of filters at $= k\,\Delta f$ with filter characteristics $W(f - f_0)$ ($= W(f_0 - f)$) to give the me results as convolution and sampling. In Fig. A.5 it is shown how the ıtput $Y(i)$ is found using the filter model (i is the time index as defined

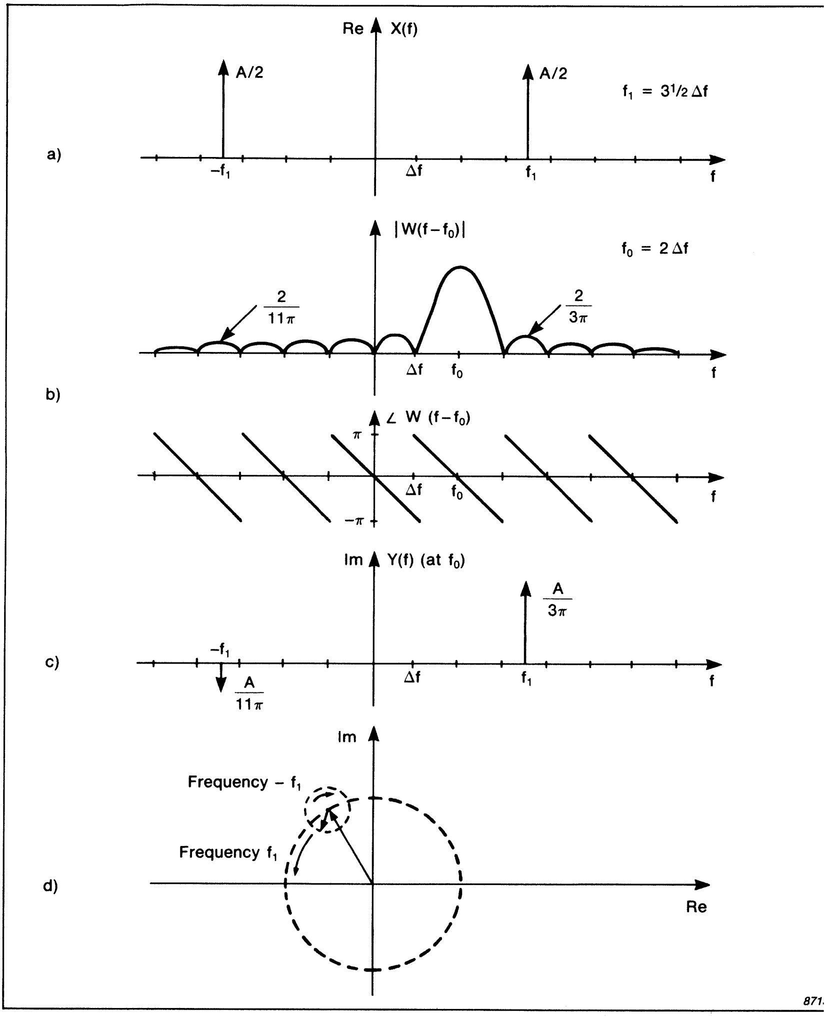

Fig. A.5. a) Spectrum of input time signal $x(t) = A \cos\left(2\pi f_1 t\right)$, $f_1 = 3\,^1\!/\!_2\;\Delta f$,
b) amplitude and phase characteristic of filter/line at $f_0 = 2\Delta f$, with rectangul weighting,
c) Spectrum of output signal for filter/line $f_0 = 2\,\Delta f$,
d) complex time output signal for filter/line $f_0 = 2\Delta f$ (sum of contra-rotating vectc with frequency of f_1 and $-f_1$ respectively)

ırlier). The input signal is in this example a cosine with frequency = $3\frac{1}{2}\,\Delta f$ and the filter considered is at $f_0 = 2\,\Delta f$ as shown in Fig. A.5 a) ıd b). The complex filter output at $f_0 = 2\,\Delta f$ in the frequency domain and ı the time domain is shown in Fig. A.5 c) and d) respectively. $|Y(i)|$ will ary between

$$|Y(i)|_{max} = \frac{A}{3\pi} + \frac{A}{11\pi} \quad \text{and} \quad |Y(i)|_{min} = \frac{A}{3\pi} - \frac{A}{11\pi}$$

ʼhich means $\dfrac{|Y(i)|_{max}}{|Y(i)|_{min}} = 1{,}75$ (corresponding to 4,9 dB).

The maxima are found when the two contra-rotating vectors point in the ame direction and the minima when they point in opposite directions.

This varying amplitude can be seen on the FFT analyzer when analyzing sinusoid with free run trigger and Rectangular weighting (see Ref. [4] 'ig. 8 for inst.).

In the other model this is explained by changing the phase of the input ignal relative to the window, i.e truncating at different points in time. 'runcating at a zero crossing of the sinusoid instead of at a maximum will ive a different tone burst and a corresponding different spectrum than hown in Fig. A.3 b). The sidelobes of the sin x/x will add at low frequencies and subtract at high frequencies instead of subtract at low frequencies nd add at high frequencies as in Fig. A.3 b). This is discussed in detail in Ref. [4].

Conclusion

The filter analogy of the FFT has been discussed and is a practical tool in nany situations to better understand certain phenomena and is used exensively in this article. The limitation in the analogy with respect to realime considerations has been pointed out as well and should be kept in nind.

The other formulation based on time multiplication – frequency convoution and sampling has proven to be a very convenient and a preferable nodel in several other applications of FFT.

It should be noted that these models or mathematical formulations are leveloped for understanding the FFT techniques. They are valid within heir limitations and neither one should be considered superior to the ther.

Appendix B

Windows and Figures of Merit

The mathematical formulation of the Weighting Functions used in th B & K Analyzers Types 2032 and 2034 is as follows:

$$w(t) = a_0 - a_1 \cdot \cos 2\pi\, t/T + a_2 \cdot \cos 4\pi\, t/T - a_3 \cdot \cos 6\pi\, t/T + a_4 \cdot \cos 8\pi\, t/T$$

$$= a_0 - \sum_{i=1}^{2} a_{(2i-1)} \cdot \cos 2\pi(2i-1)\, t/T + \sum_{i=1}^{2} a_{(2i)} \cdot \cos 2\pi(2i)\, t/T \quad \text{(B.1)}$$

$$\text{for} \quad 0 \leqq t < T$$

$$w(t) = 0 \qquad \text{elsewhere}$$

except for Transient and Exponential Weighting.

As can be seen the windows consist of a sum of a DC and four harmoni terms. The coefficients of the 4 standard windows implemented in th 2032 and 2034 are given in Table B.1.

	a_0	a_1	a_2	a_3	a_4
Rectangular	1	–	–	–	–
Hanning	1	1	–	–	–
Kaiser-Bessel	1	1,298	0,244	0,003	–
Flat Top	1	1,933	1,286	0,388	0,032

T01601GI

Table B.1. Window coefficients

Maximum Amplitude

The max. amplitude can be calculated from the sum of the window coefficients.

$$\text{Max } w(t) = \sum_{i=0}^{n} a_i \quad \text{(B.2)}$$

ınother relevant quantity for windows, sometimes called the Coherent in, is

$$\text{ıerent Gain} = a_0 / \text{Max } w(t) \tag{B.3}$$

Γhis quantity indicates the reference amplitude gain of the filter char- ,eristic if the maximum amplitude (Max. $w(t)$) was unity.

.n 2032/34 all windows are scaled in such a manner that the "area" un- : the weighting function is equal to one ($a_0 = 1$). This corresponds to a 'erence gain of unity which ensures no power spectral bias error for a ıusoid with a frequency coinciding with one of the centre frequencies/ es of the filters.

ffective Duration

ıe effective duration of the window is calculated from

$$_{\text{ff}} = \frac{1}{(\text{Max } w(t))^2} \int_0^T w^2(t)\, dt \tag{B.4}$$

By use of (B.2) and Parseval's theorem, for the weighting function con- lered as a periodic function with period T, the effective duration can be lculated from the square of the window coefficients by

$$_{\text{eff}} = \frac{a_0^2 + 2\sum_{i=1}^{n} \left(\frac{a_i}{2}\right)^2}{\left(\sum_{i=0}^{n} a_i\right)^2} \cdot T \tag{B.5}$$

The effective duration can be interpreted as a measure of the energy ntegral of values squared) of the weighting function $w(t)$ normalized ith the maximum amplitude Max. $w(t)$.

ːffective Noise Bandwidth

'he Effective Noise Bandwidth (ENBW) is defined as

$$\text{ːNBW} = \frac{\int_{-\infty}^{\infty} |W(f)|^2\, df}{\text{Max } |W(f)|^2} \tag{B.6}$$

Using Parseval's theorem we find the definition in the time domain giv en by

$$\text{ENBW} = \frac{\int_0^T w^2(t)\,dt}{\left(\int_0^T w(t)\,dt\right)^2} \tag{B.7}$$

Again using Parseval's theorem for the weighting function considered as periodic function with period T as previously we find, since

$$\int_0^T w(t)\;dt = a_0 T \tag{B.8}$$

that

$$\text{ENBW} = \frac{\left(a_0^2 + 2\sum_{i=1}^{n}\left(\frac{a_i}{2}\right)^2\right)T}{a_0^2 T^2} = \frac{a_0^2 + 2\sum_{i=1}^{n}\left(\frac{a_i}{2}\right)^2}{a_0^2}\cdot\Delta f \tag{B.9}$$

The reciprocal of ENBW is sometimes in the literature called the Pro cessing Gain (PG), since an increased noise bandwidth permits additiona noise to contribute to a spectral estimate, giving a lower signal to nois ratio, when detecting sinusoidal signals in noise.

Overlap Correlation

If windows are applied to non-overlapping partitions of a time sequence, a significant part of the time signal is ignored due to the fact that most win dows exhibit small values near the boundaries. To avoid this loss of data overlap analysis can be performed.

In 2032/34 standard overlap of 0%, 50%, 75% and maximum can be chosen.

The correlation as a function of fractional overlap, r can be calculated using the correlation coefficient.

$$c(r) = \frac{\int_0^T w(t)\cdot w\Big(t+(1-r)\,T\Big)\,dt}{\int_0^T w^2(t)\,dt} \tag{B.10}$$

Correlation Coefficient	25% Overlap	50% Overlap	75% Overlap	100% Overlap
Rectangular	0,25	0,5	0,75	1
Hanning	0,0075	0,1667	0,6592	1
Kaiser-Bessel	0,0014	0,0735	0,5389	1
Flat Top	0,0005	– 0,0153	0,0455	1

T01602GB0

ble B.2. Correlation coefficients for 25%, 50%, 75% and 100% overlap for the various ıdow functions

The correlation coefficients for 25%, 50%, 75% and 100% overlap are own in Table B.2.

For an estimate based on the average of a number n_d of statistically in- pendent records (or degrees of freedom) the BT-product (Bandwidth nes Averaging Time) per filter is equal to the number of averages inde- ndent of the weighting function used

$$T = n_d \tag{B.11}$$

Thus the relative standard deviation, ϵ_r for autospectra (RMS) of gauss- n random signals is

$$= \frac{1}{2\sqrt{BT}} = \frac{1}{2\sqrt{n_d}} \tag{B.12}$$

In an analysis with average of n_d records with 50% overlap the BT-prod- t is given by (Refs. [2 and 3])

$$T_{50\%} = \left[[1 + 2c^2(50\%)]/n_d - 2c^2(50\%)/n^2{}_d \right]^{-1} \tag{B.13}$$

ıd for 75% overlap the BT-product is given by (Refs. [2 and 3]).

$$T_{75\%} = \left[[1 + 2c^2(75\%) + 2c^2(50\%) + 2c^2(25\%)]/n_d \right.$$

$$\left. 2[c^2(75\%) + c^2(50\%) + 3c^2(25\%)]/n^2{}_d \right]^{-1} \tag{B.14}$$

The negative terms in B.13 and B.14 are edge effects of the average and n be ignored if the number of averages, n_d is larger than ten. Also note that for most windows the correlation (squared) for 25% overlap is sma compared to 1 and can also be omitted from B.14 without significant erro

The effective BT-product per filter per record $BT_{eff.}$ shown in Table (in Part I of this article) is now calculated from

$$BT_{eff}\,(50\%) = BT_{50\%}\,/n_d \qquad \text{(B.15}$$

and

$$BT_{eff}\,(75\%) = BT_{75\%}\,/n_d \qquad \text{(B.16}$$

The theoretical values have been verified experimentally (see **Appendix D**).

An example: for a white noise gaussian random signal 123 spectra hav been averaged using Hanning Weighting with 75% overlap. What is th difference in dB between the maximum and minimum values in the auto spectrum estimate?

From Table 3 we have the effective BT-product to be 123 · 0,52 = 64 From (B.12) the relative standard deviation (68% confidence interval) i 1/16 or 0,5 dB. The 99% confidence interval is given by ± three times th standard deviation. Assuming that the maximum and minimum values o the spectral estimate will be the extremes of the 99% confidence interva we will have a difference between the maximum and minimum values o $2 \cdot 3 \cdot \epsilon_r$, i.e. here 3 dB.

Appendix C

ꞒEffective Weighting of)verlapped Spectral Averaging

'he effective weighting of an overlapped spectral average analysis can be efined as the variation of the spectral level from an impulse versus the npulse's position in time – that is the weight given to the data in the pectral average as a function of time. For example, for 50% overlap, linar averaging and Hanning window a weighting as shown in Fig. C.1 is btained. The Figure of interest here is the ripple on the spectral level, 'hich can be defined as 10 log (Max/Min) – in the above example 3 dB.

The effective weighting is relatively easy to calculate numerically by umming a series of squared weighting functions with the specified overıp (see **Appendix A** eqn. (A.16)). The ripple periodicity must by symıetry be the same as the shift between spectra.

A case of interest is the effective weighting function obtained in overlap nalysis with Hanning window applied. The ripple obtained as a function f shift between records is shown in Fig. C.2. As can be seen the ripple falls ery rapidly from 3 dB for a shift of 0,5 to zero between shifts of 0,3 and ,4. Additional zeroes are seen for smaller shifts. These actually lie in the eries 1/3, 1/4, 1/5 1/6 etc., i.e. 1/(integer>2).

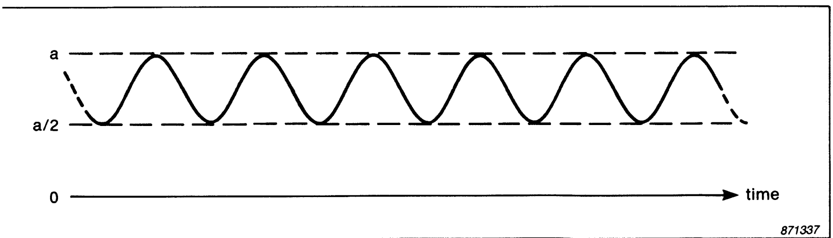

ig. C.1. Ripple in the effective weighting of the time signal when using Hanning Weightıg and 50% overlap

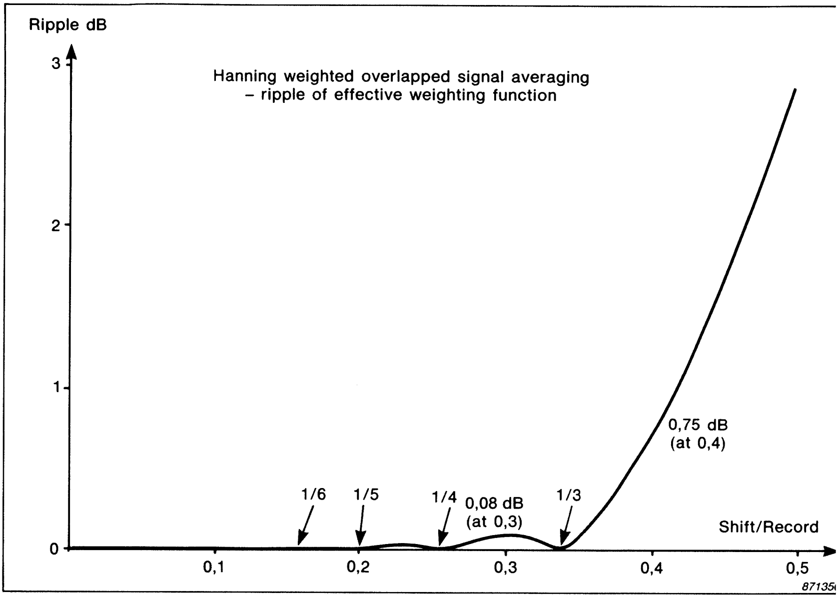

Fig. C.2. Ripple of effective weighting function using Hanning weighted overlapped sig nal averaging

Among other things this means that the widest analysis bandwidth fo overlapped averaging to obtain a uniform weighting is found with an over lap of 2/3. While 2/3 is not a practical shift given the normal FFT size th nearest value is quite good enough.

This situation comes about in the following manner. The squared Han ning has a form $[1 - \cos(2\pi\, {}^{t}/_{T})]^2$, i.e. contains only a constant and th terms $\cos(2\pi t/T)$ and $\cos(4\pi t/T)$, where T is the window length. Th shift of the window is equivalent to a phase shift of A for the $\cos(2\pi t/T$ term and $2A$ for the $\cos(4\pi t/T)$ term. Considering the series of window which affect a given impulse, the ripple is contained in these cos terms an the contribution for each term can be considered as the real part of a com plex addition – the example for two windows separated by A is shown i Fig. C.3.a.

It is seen in Fig. C.3.b that when the shift is 0,5 of the window length, i.e the phase shift $A = \pi$, the sum of only the terms with phase difference A i zero.

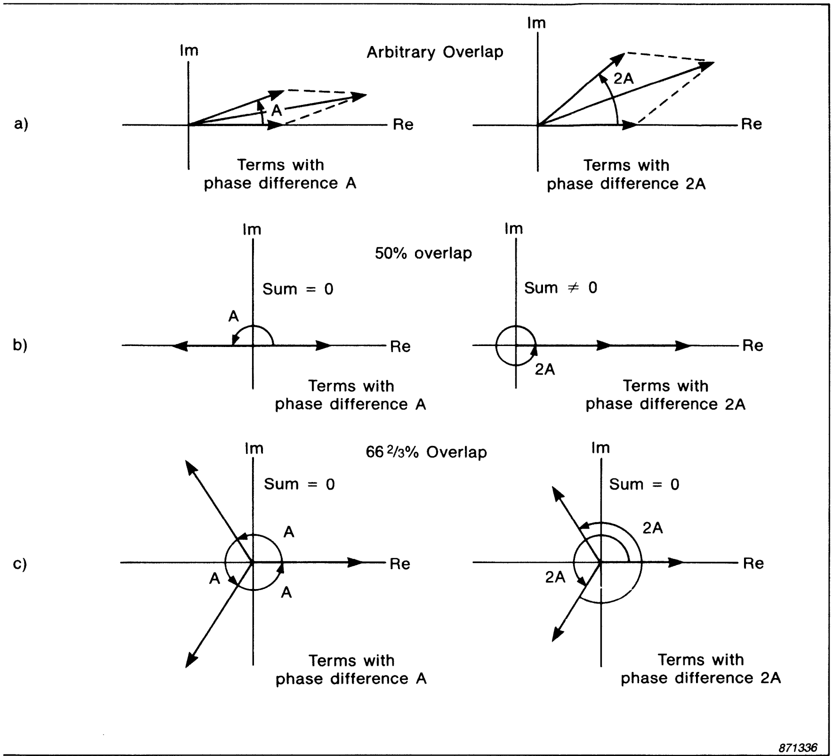

'ig. C.3. Addition (complex) of the terms with phase difference A and 2A in calculation f the ripple of the effective weighting function in situation with overlapping and Ianning

But when a shift of 1/3 is used the sum of both the terms with phase lifference A and $2A$ are zero and likewise for any shift of 1/(integer>2).

Thus the overlap must be 2/3, 3/4, 4/5, 5/6 etc. (see Fig. C.4) to obtain re- ults equivalent to a true real-time analysis with parallel filters (Refs. [1, 5 ınd 6] and **Appendix A**).

75% overlap is the most commonly used overlap, since it is an integer ıumber of samples when the transform size is a power of two.

Using special parameter number 2 in 2032/34 an overlap of 1365 samples :orresponding to nearly 2/3 record length can be specified, thus giving a ıearly flat weighting in the widest analysis bandwidth possible.

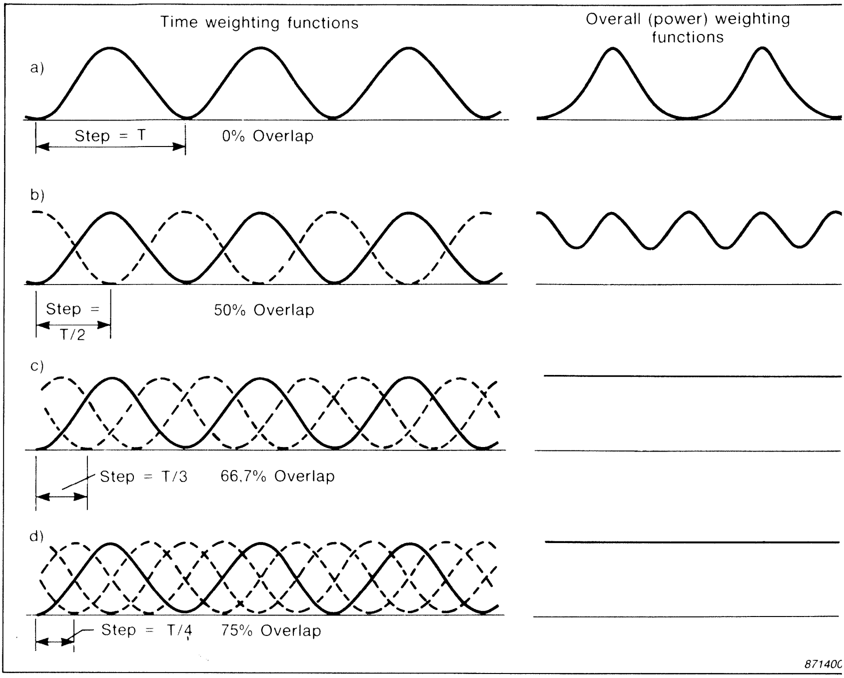

Fig. C.4. Overall weighting functions for overlapping Hanning windows

Appendix D

Experimental Determination of the BT-Product for FFT-Analysis using different weighting functions and overlap

The BT-product is determined from the relative standard deviation, ϵ_r of he amplitude of auto-spectra estimates when analyzing a gaussian white noise random signal.

For RMS values we have

$$\epsilon_r = \frac{1}{2 \cdot \sqrt{BT}} \Leftrightarrow BT = \frac{1}{4 \cdot \epsilon^2_r} \qquad (D.1)$$

which means that we can determine the BT-product from experimentally etermined standard deviations of autospectra estimates (measure- ments). The effective BT-product per record BT_{eff} is then given by

$$BT_{eff} = \frac{BT}{n_d} \qquad (D.2)$$

where n_d is number of linear averages.

The Measurement Setup is shown in Fig. D.1.

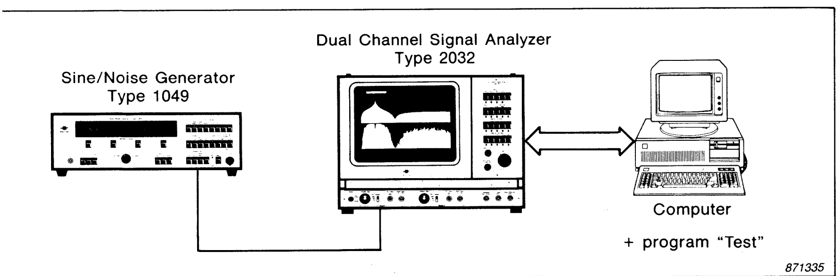

Fig. D.1. The instrumentation for experimental determination of the BT-product for FFT analysis

BT_{eff} per record	0% Overlap	50% Overlap	75% Overlap
Rectangular	0,954	0,674	0,368
Hanning	0,995	0,940	0,535
Kaiser-Bessel	1,009	0,996	0,628
Flat Top	0,990	1,000	0,994

T01603GB

Table D.1. Effective BT-product per record, when overlap analysis is performed (experimental values)

The number of averages (LIN), the overlap and the weighting functior are chosen in the Measurement Setup of the 2032.

The readout of absolute (RMS) or relative (dB) values are chosen in th(Display Setup.

The frequency interval (number of lines) and the number of estimate: (measurements) are chosen in the programme.

Now the mean values and standard deviations from the autospectra a1 each frequency in the chosen frequency interval, as well as the mean valu(of these mean values and standard deviations are calculated in th(computer.

A typical result is taken as the mean value of four experiments. In eacł experiment 100 estimates of autospectra, using 100 averages and 40 frequency lines, have been taken. Most of the results shown in Table D.1 agree within 1 % of the theoretical values shown in Table 3 in Part I of thi: article.

Appendix E

Examples of User Defined Windows

The User Defined windows are implemented in the B & K Analyzers Types 2032/34 as

$$W(n) = \frac{2^{E}}{32768}\left[A_0 - A_1\cos\left(n\frac{2\pi}{N}\right) + A_2\cos\left(2n\frac{2\pi}{N}\right) - A_3\cos\left(3n\frac{2\pi}{N}\right)\right.$$

$$\left. + A_4\left(4n\frac{2\pi}{N}\right)\right] \qquad \text{(E.1)}$$

$0 \leqslant n \leqslant N-1$

N = 1024 if in Zero Pad Mode
N = 2048 if not in Zero Pad mode

Notice the slightly different formulation from the rest of this article with a common scaling factor for all the window coefficients.

In the design of User Defined windows the following criterion must be used:

The exponent E must be an integer as small as possible, however large enough to fulfil Equation (E.2).

$$2^{E} \geqq \sum_{i=0}^{n} a_i \qquad \text{(E.2)}$$

The coefficients A_i (E.1) are now calculated

$$A_i = 2^{(15-E)} \cdot a_i \qquad \text{(E.3)}$$

Hamming Window

The Hamming window is defined as

$$w(t) = 1 - 0{,}84 \cos\left(2\pi \frac{t}{T}\right) \quad \text{for } 0 \leqslant t < T$$

$$w(t) = 0 \qquad \text{elsewhere} \qquad \text{(E.4}$$

and has an Effecitve Noise Bandwidth of 1,3528 Δf.

The Hamming window can be implemented in the 2032 or 2034 usin special parameters #6 to #12.

First the Noise Bandwidth is entered in special parameters #6 to #9 a

6 and #8: 13528.
7 and #9: –4.

Then the common exponent E in

10: 1.

And finally the coefficients, here A_0 and A_1 in

11: 2^{14} = 16384 and
12: $2^{14} \cdot 0{,}84$ = 13762.

This window is very similar to the Hanning Window, but has the specia feature, that it suppresses the first sidelobe. However, the fall-off rate o the side-lobes is only 20 dB per decade compared to 60 dB per decade fo the Hanning window. Fig. E.1 a) shows a "worst case" analysis of a sinusoi with Hamming weighting.

Blackman-Harris Window

The four term −92 dB Blackman-Harris window has the followin coefficients:

$a_0 = 1$, $a_1 = 1{,}36...$, $a_2 = 0{,}39...$, $a_3 = 0{,}032...$. The Effective Noise Bandwidt is 2,00.. Δf.

The window is implemented in the 2032 or 2034 using the special param eters #6 to #14 as

#6 and #8: 2.
#7 and #9: 0.
#10: = 2.
#11: 2^{13} = 8192.
#12: $2^{13} \cdot 1{,}36$ = 11150.
#13: $2^{13} \cdot 0{,}39$ = 3226.
#10: $2^{13} \cdot 0{,}032$ = 267.

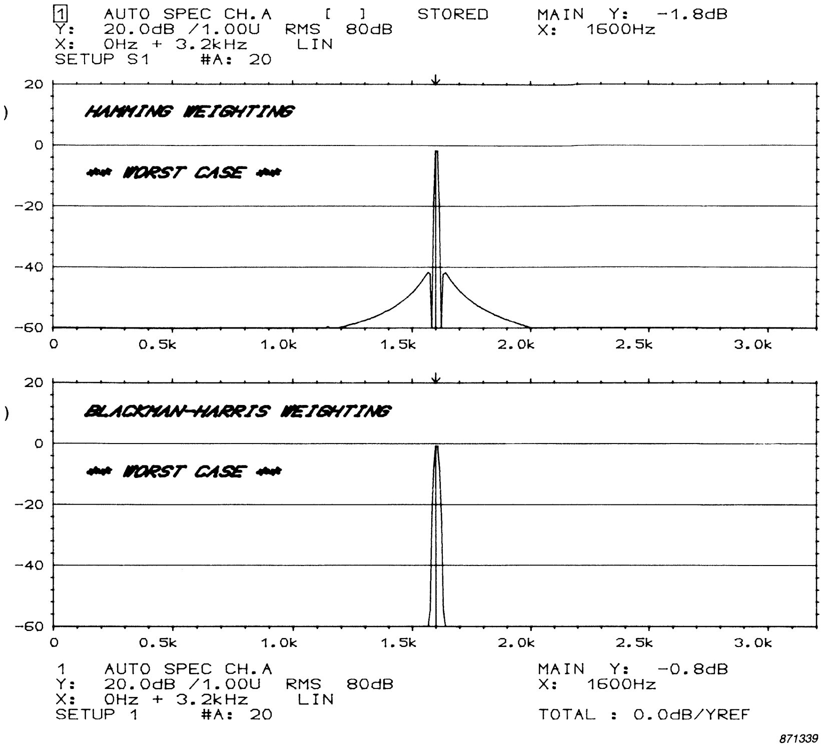

g. E.1. The "worst case", when analysing a sinusoid using a) Hamming window and Blackman-Harris window

The Blackman-Harris window has very much the same performance as ıe Kaiser-Bessel window Ref. [2] except that it suppresses the sidelobes ıore than 92 dB at a cost of an 11% wider Noise Bandwidth. In Fig. E.1 b) "worst case" analysis of a sinusoid with Blackman-Harris weighting is ıown.

Appendix F

Picket Fence Effect

Whenever analysis with discrete fixed filters is performed, the spectrum i measured at the filter centre frequencies with a resolution given by th filter bandwidths. This is not only the case for DFT/FFT analysis, but i general when a bank of parallel filters or stepped filters are used for th analysis.

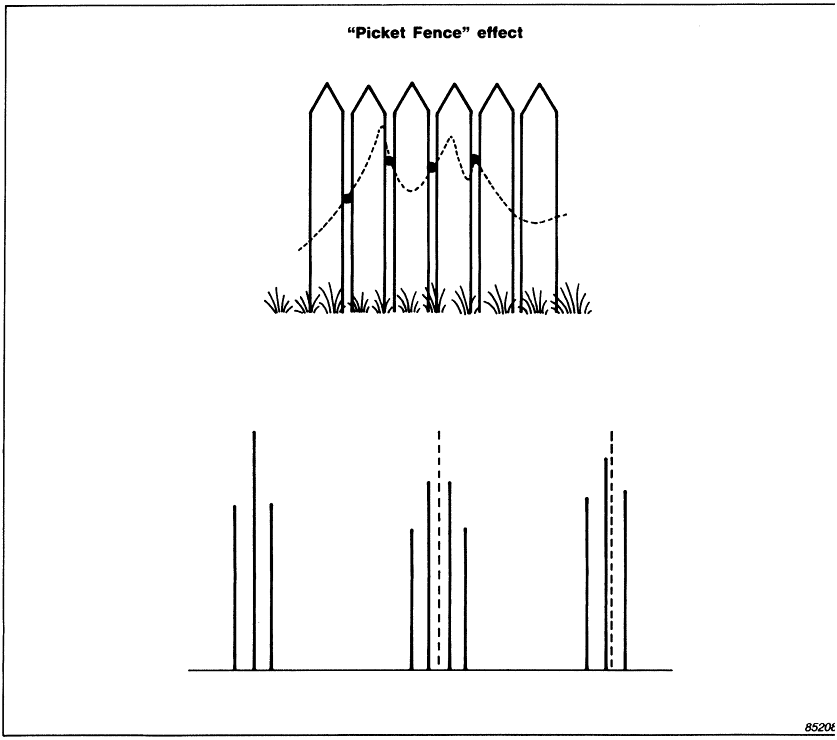

Fig. F.1. Illustration of Picket Fence Effect

The effect of only measuring the spectrum at discrete frequencies is re-
rred to as the picket fence effect, since it is similar to viewing the contin-
ous spectrum (measured with the given bandwidth) through a picket
nce, see Fig. F.1.

As indicated in Figs. 7, 9, 12 and 16 (shown in Part I of this article) we
ill therefore in general get an error in both amplitude and frequency of
ie highest line in the spectrum of a frequency component. The amplitude
rror is limited by the ripple in the passband while the frequency error is
mited by the line spacing Δf. The errors are referred to as picket fence
ffect errors. Only in the situation where the frequency component coin-
ides with a centre frequency/line in the analysis both the amplitude and
ie frequency will be correct.

If we know or assume that it is a single and stable frequency component
ie errors can be compensated for by an interpolation technique on the
ell defined filter characteristics of the weighting functions, see Figs. 6, 8,
1 and 15 (in Part I of this article). The amplitude and frequency correc-
ons can be calculated from the difference Δ, in dB, between the two high-
st lines around the peak. We will here limit the discussion to the Hanning
indow and Rectangular window, but similar formulae could be devel-
ped for other window functions.

The frequency correction, Δf_c Hz for Hanning Weighting is given by:

$$f_c = \frac{2-10^{\Delta \mathrm{dB}/20\ \mathrm{dB}}}{1+10^{\Delta \mathrm{dB}/20\ \mathrm{dB}}} \cdot \Delta f \qquad \text{(F.1)}$$

here Δf is the line spacing in the analysis.

The Equation F.1 is shown in graphical form in Fig. F.2 and is tabulated
n Table F.1.

For Hanning Weighting, ΔdB has a maximum of 6 dB, when the fre-
uency coincides exactly with an analysis line, and a minimum of zero dB,
hen it falls exactly between two lines.

The amplitude correction, ΔL dB for Hanning Weighting is given by

$$\Delta L = 20 \log \left| \frac{\sin \pi \Delta f_c / \Delta f}{\pi \Delta f_c / \Delta f} \cdot \frac{1}{1-(\Delta f_c/\Delta f)^2} \right| \qquad \text{(F.2)}$$

hich is also shown in graphical forms in Fig. F.2 and is tabulated in
able F.1.

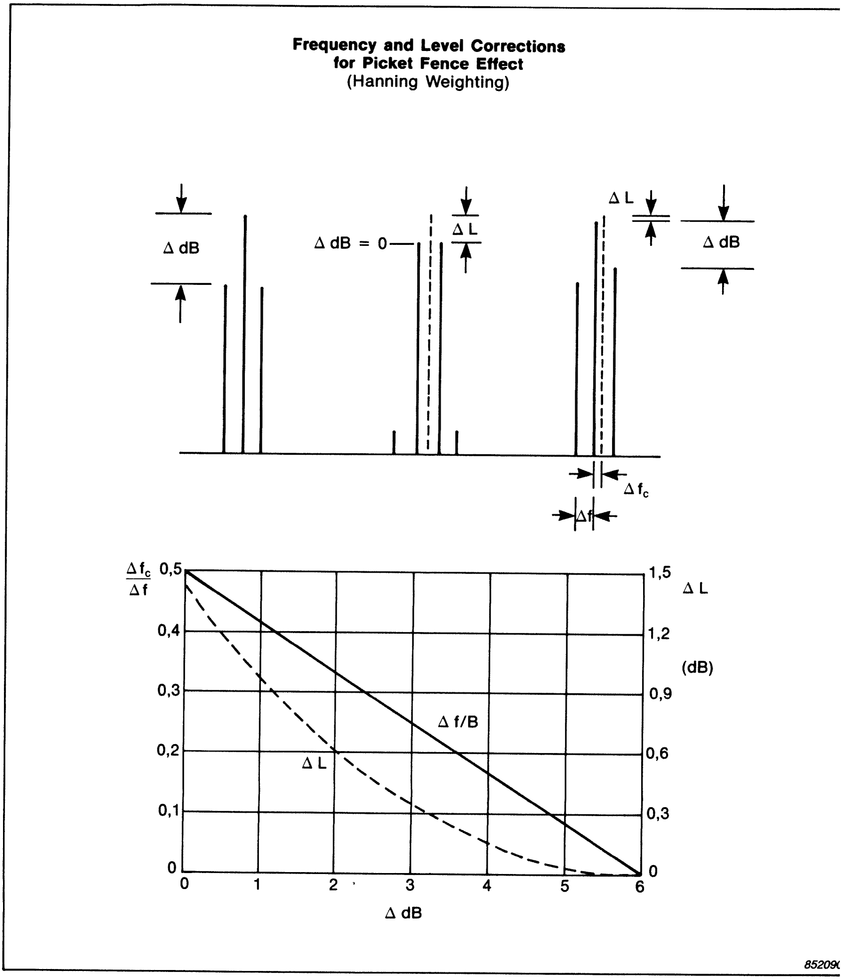

Fig. F.2. Amplitude and frequency compensation for picket fence effect with Hanning Weighting

For Hanning Weighting the amplitude correction, ΔL is 0 dB, when the frequency coincides exactly with an analysis line, which is indicated by a ΔdB equal to 6,0 dB. The amplitude correction is 1,42 dB, when ΔdB is equal to 0 dB, that is when the frequency of the signal is exactly between two lines.

ΔdB	ΔL	Δf_c	ΔdB	ΔL	Δf_c
0.0	1.42	0.50	3.0	0.33	0.24
0.2	1.33	0.48	3.2	0.29	0.23
0.4	1.23	0.47	3.4	0.25	0.21
0.6	1.14	0.45	3.6	0.21	0.19
0.8	1.05	0.43	3.8	0.18	0.18
1.0	0.97	0.41	4.0	0.14	0.16
1.2	0.89	0.40	4.2	0.12	0.14
1.4	0.81	0.38	4.4	0.09	0.13
1.6	0.74	0.36	4.6	0.07	0.11
1.8	0.67	0.35	4.8	0.05	0.10
2.0	0.61	0.33	5.0	0.04	0.08
2.2	0.55	0.31	5.2	0.02	0.06
2.4	0.49	0.29	5.4	0.01	0.05
2.6	0.43	0.28	5.6	0.01	0.03
2.8	0.38	0.26	5.8	0.00	0.02
			6.0	0.00	0.00

T01648GB0

ıble F.1. Amplitude and frequency compensation for Picket Fence Effect with Hanning 'eighting

Using this picket fence correction technique it is possible to achieve a :equency accuracy approximately 100 times finer than the line spacing. 'or cursor read out on 2032/34 the dB values used for these calculations an be found with two decimals rather than one in the Scratch Pad Memoy octal addresses 1257 (the integer) and 1260 (the 10-exponent) for the .pper graph, and 1357 (the integer) and 1360 (the 10-exponent) for the ɔwer graph, see Fig. F.3.

For Rectangular Weighting the corresponding correction terms are for requency

$$\Delta f_c = \frac{1}{1 + 10^{(\Delta dB/20\ dB)}} \cdot \Delta f \qquad (F.3)$$

nd for amplitude

$$\Delta L = 20 \log \left| \frac{\sin \pi\ \Delta f_c / \Delta f}{\pi \Delta f_c / \Delta f} \right| \qquad (F.4)$$

'or system analysis where identification of resonance frequencies and lampings are essential similar techniques can be used. For lightly damped ıtructures it is assumed that a resonance peak can be modelled by a single

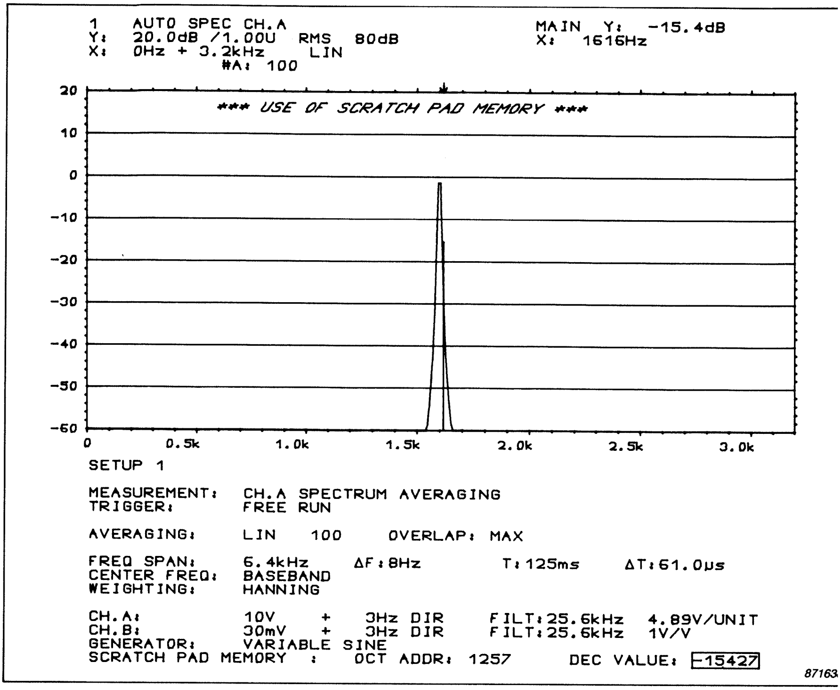

Fig. F.3. The use of scratch pad memory for readout of cursor values with highe accuracy

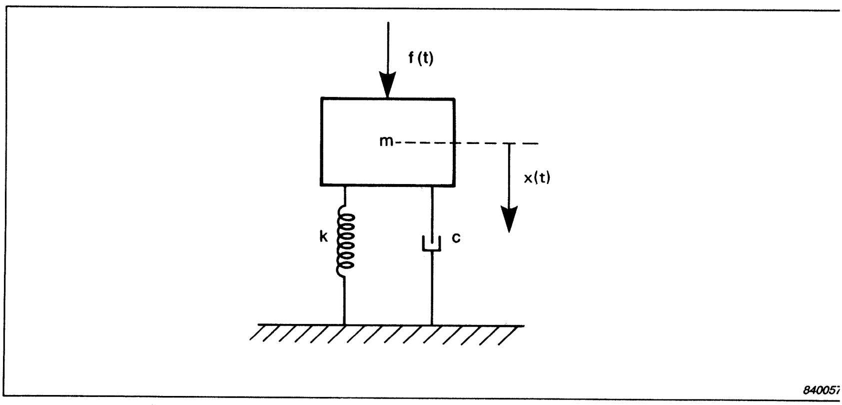

Fig. F.4. Mechanical Single Degree of Freedom (SDOF) model ɘgree of freedom (SDOF) model, see Fig. 4. Such a model, consisting of a .ass, spring and a damper (Refs. [9 and 10]) has a Frequency Response ınction as shown in Fig. F.5.

Using a curvefit technique where the mathematical SDOF model is fit- d to the measured Frequency Response Function using the method of ast squares error, the resonance frequency, the peak amplitude and the ımping can be estimated with a degree of accuracy much better than the solution of the FFT analysis allows. The assumption is that the mea- ırement is free of leakage.

An example is shown in Fig. F.6 where the resolution, i.e. the line spac- g is 4 Hz. Pseudo-random excitation is here used to avoid leakage in the ıalysis. The curvefit calculates the resonance frequency with a resolution ; least 100 times higher than the FFT analysis. A zoom measurement ɘrifies the results.

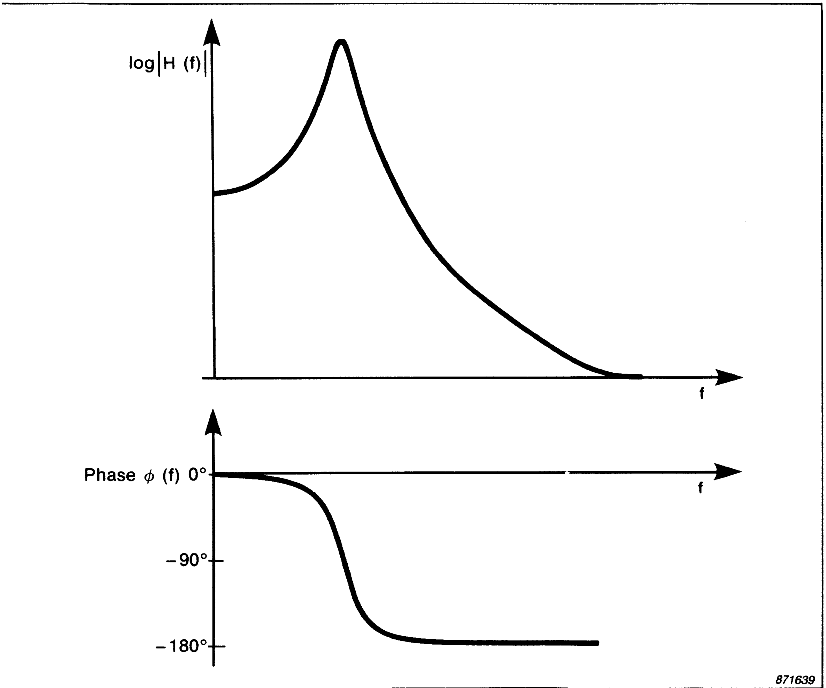

g. F.5. Logarithmic amplitude log | H(f) | and phase ϕ(f) of the Frequency Response ınction of a Single Degree of Freedom model

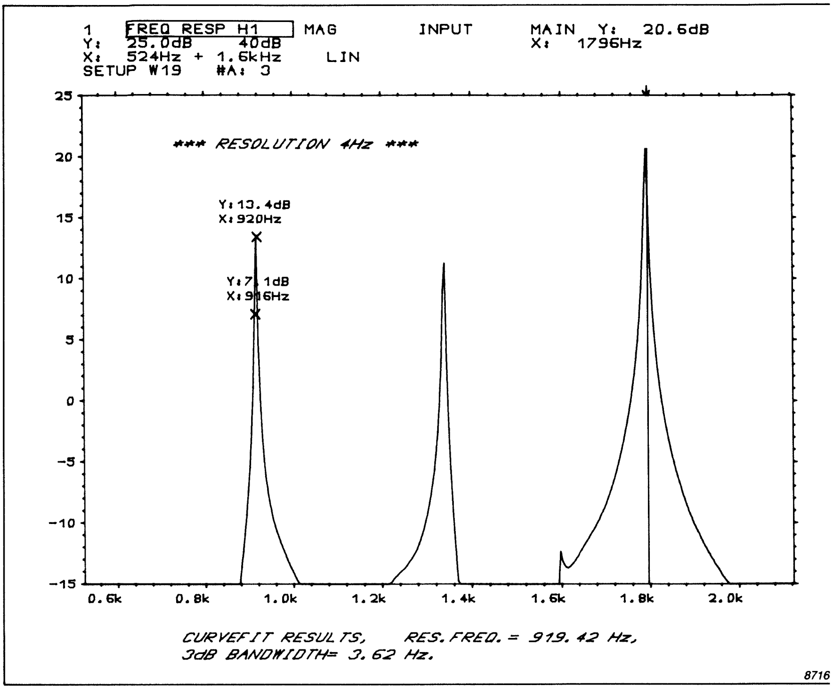

Fig. F.6. Estimation of resonance frequency and 3 dB bandwidth using a curvefit tech nique. Note that the line spacing in the analysis, Δf is 4 Hz

References

[1] Randall, R.B. "*Frequency Analysis*", Brüel & Kjær, 1987

[2] Harris, F.J. "*On the Use of Windows for Harmonic Analysis wit the Discrete Fourier Transform*", Proceedings of th IEEE, Vol. 66, No.1, January 1978, pp. 51–83.

[3] Welch, P.D. "*The use of Fast Fourier Transform for the estima tion of power spectra: A method based on time averag ing over short, modified periodigrams*", IEEE Tran Audio Electro Acoust., Vol. AU–15, June 196 pp.70–73

4] Thrane, N. "*The Discrete Fourier Transform and FFT Analyzers*", B & K Technical Review, No.1–1979

5] Thrane, N. "*Zoom FFT*", B & K Technical Review, No.2–1980

6] Boyes, J.D. "*Effective Weighting of Overlapped Spectral Averaging*", B & K Internal Paper, 1980

7] Brigham, E.O. "*The Fast Fourier Transform*", Prentice Hall Inc., New Jersey, 1974

8] Papoulis, A. "*The Fourier Integral and its Applications*", McGraw-Hill Inc., New York, 1962

9] Herlufsen, H. "*Dual Channel FFT Analysis, Part 1*", B & K Technical Review, No.1–1984

0] Herlufsen, H. "*Dual Channel FFT Analysis, Part 2*", B & K Technical Review, No.2–1984

'ootnote *(from page 7)*

The linear averaging algorithm used in the analyzers is:

$$\overline{Y(i)}|^2 = \frac{1}{i}\,|Y(i)|^2 + \frac{i-1}{i}\,|\overline{Y(i-1)}|^2$$

›r $1 \leqslant i \leqslant N$

'hus the averaging can be stopped with correctly scaled result after any umber of averages without having to wait for the predefined number of ·erages, N, to be performed.

Acoustic Calibrator for Intensity Measurement Systems *

by Erling Frederiksen

Abstract

A description is given of an acoustic calibrator for intensity measuremen systems which use microphones of the pressure principle. The calibratc produces signals corresponding to those detected by intensity probe mi crophones when the probe is placed in a free progressive sound wave wit either 0° or 90° incidence.

In the 90°-mode the signals of the calibrator are equal with respect t magnitude and phase. This mode can be used for pressure-sensitivity cali bration of intensity systems and for measurement of residual intensity ir dex. Calibrators supplying this type of signals have previously been de scribed in the literature.

However, for a more rigorous calibration it should be verified that th system responds correctly also to a phase difference between the soun field signals when this differs from zero. Therefore this calibrator has als the 0°-incidence mode. In this mode the calibrator signals are equal to th signals at two points in space within a free progressive sound wave. Th phase difference corresponds to a certain distance between the point which means that it is proportional to frequency. The signal magnitude and the phase difference have revealed high stability and calibration accu racy of 0,1 dB is possible. The calibrator can also be used for particle ve locity calibration.

Sommaire

Tout d'abord la description d'une source sonore étalon pour les système de mesure d'intensité acoustique par microphones sensibles à la pressio

* First published in Internoise 1987

t donnée. Cette source produit des signaux correspondant à ceux qui nt détectés par les microphones des sondes, lorsque la sonde est exposée une onde sonore progressive libre avec une incidence de 0 ou de 90°.

Dans le mode 90°, les signaux de la source sont identiques en amplitude phase. Ce mode peut être utilisé pour l'étalonnage de sensibilité en pres-on des systèmes d'intensité et pour les mesures d'index d'intensité rési-ıelle. Des sources délivrant ce type de signal ont déjà été décrites dans la ,térature.

Cependant, pour un étalonnage plus rigoureux, il faut vérifier que le sys-me répond correctement lorsqu'il y a une différence de phase entre les ,ux signaux. C'est pour cela que la source dispose d'un mode 0°, où les gnaux provenant de la source sont identiques aux signaux engendrés en ,ux points de l'espace par une onde sonore progressive libre. La différen- de phase correspond à une distance donnée entre les points, et elle est onc proportionnelle à la fréquence. L'amplitude des signaux et les diffé-nces de phase ont révélé qu'une très grande stabilité et qu'une précision 0,1 dB sont possibles. La source peut aussi être utilisée pour les étalon-ıges de vitesse particulaire.

usammenfassung

Es wird ein akustischer Kalibrator für Intensitätsmeßsysteme mit ruckmikrofonen beschrieben. Das vom Kalibrator erzeugte Signal en-pricht dem von einer Intensitätssonde aufgenommenen, wenn sich dieses einem freien Schallfeld mit 0°- oder 90°-Einfall befindet.

Beim 90°-Betrieb erzeugt der Kalibrator Signale, die nach Betrag und hase gleich sind. Hiermit läßt sich der Druckübertragungsfaktor des In-nsitätsmeßsystems kalibrieren sowie der Remanenz-Intensitätsindex estimmen. Kalibratoren, die diese Signalart erzeugen, wurden bereits üher in der Literatur beschrieben.

Für eine strengere Überprüfung der Kalibrierung sollte auch das Verhal-n bei Signalen, die eine unterschiedliche Phasenlage besitzen, unter-ıcht werden. Hierfür besitzt der Kalibrator den 0°-Betrieb. Hier erzeugt er Kalibrator Signale, die den Signalen an zwei räumlich verschiedenen tellen einer sich frei fortpflanzenden Schallwelle entsprechen. Die Pha-ndifferenz entspricht einem gegebenen Abstand im Raum, d.h. sie ist equenzproportional. Der Betrag und die Phasendifferenz der Signale nd hochstabil und eine Kalibriergenauigkeit von 0,1 dB ist möglich. Der alibrator läßt sich auch zur Teilchenschnelle-Kalibrierung einsetzen.

Introduction

Today measurement of sound intensity has proved its usefulness for noi analysis. Instruments are constantly improving, but as they are quite cor plex many users have desired means of calibration to gain further con dence in their measurement results.

Most systems use pressure microphones and practically all field calibr tions made today are pressure calibrations of the system channels. In few cases the channels are also tested for equality of their phase responses usually at one frequency only.

An acoustical calibrator for a far more extended calibration has be developed. According to known principles it can be used for pressure lev calibration at 250 Hz and for phase check by measurement of residual i tensity index between 10 Hz and 5 kHz.

In addition to these features the calibrator has an extra operation mo in which it produces signals for calibration of intensity and particle velo ty sensitivity of instruments operated in these modes. This new mode the main theme of this paper.

Operation Principle of Intensity System with Pressu Microphones

Most measurement systems which employ pressure microphones dete mine the instantaneous values of particle velocity, $u(t)$ and of the sour intensity, $I(t)$ in accordance with the following expressions:

$$u(t) = \int \frac{p_1(t) - p_2(t)}{\rho_o \Delta r_o} dt\,; \quad I(t) = \frac{p_1(t) + p_2(t)}{2} \int \frac{p_1(t) - p_2(t)}{\rho_o \Delta r_o} d$$

$p_1(t), p_2(t)$: instantaneous values of the pressure signals
$\Delta r_o, \rho_o$: system parameters for microphone distance and air densi

For sinusoidal signals the measured values of the particle velocit $u[\text{rms}]$ and of the time average value of sound intensity, $\bar{I}$ become:

$$u[\text{rms}] = \frac{\left(\left[(P_1 + P_2)\sin\phi/2\right]^2 + \left[(P_1 - P_2)\cos\phi/2\right]^2\right)^{0,5}}{\omega\,\rho_o\,\Delta r_o}$$

$$\bar{I} = \frac{P_1 P_2 \sin\phi}{\omega\,\rho_o\,\Delta r_o}$$

, P_2: rms-values of the sinusoidal pressure signals
ω: phase angle between the pressure signals and angular frequency

peration of the Sound Intensity Calibrator

ie formulae above show that the measurement results are functions of ır signal parameters. Therefore a calibrator has to produce signals for ıich these parameters are stable as functions of time and perform in a edictable way under common environmental conditions.

A calibrator which statisfies these requirements has been developed. It nsists of a sound source and of a special coupler with two cavities, (a) d (b), see Fig. 1. The cavities have ports (1, 2 and 3) for connection of ;ensity probe microphones. One of the cavities (a) is directly connected the source while the second cavity (b) is coupled to (a) via an acoustical upling element which contains a resistance and a mass in series nnection.

At low frequencies the acoustical network formed by the coupling eleənt and by the compliance of cavity (b) creates cavity signals with a ıase difference which is proportional to frequency and with magnitudes ıich are nearly equal. These properties exactly comply with the pressure two points in a space where a plane sound wave is propagating. Thus for ɔressure microphone probe the calibrator can simulate a free field wave th definable levels of sound pressure, particle velocity and intensity.

The coupler has been designed to create a phase difference correspondg to that valid for 50 mm microphone distance with an angle of zero deees between the probe axis and the wave's propagation direction. The upler properties are independent of the choice of sound source but a well fined source is needed for sensitivity calibration, therefore a piston-

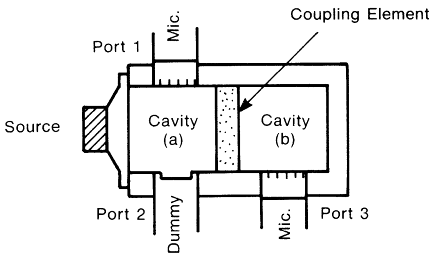

;. 1. Principle of the intensity calibrator. The microphones are placed in the ports (1) d (3) for calibration of intensity sensitivity

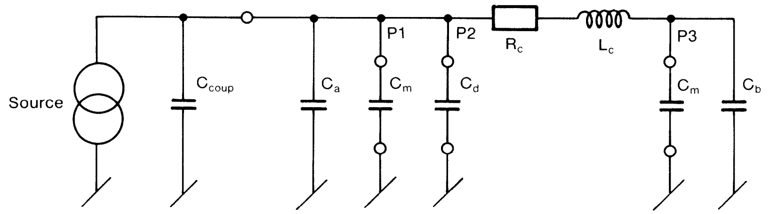

C_a:	Compliance of cavity(a)	$6{,}9 \times 10^{-11} m^5/N$	$(9{,}8 \times 10^{-6} m^3)$
C_b:	Compliance of cavity(b)	$7{,}6 \times 10^{-11} m^5/N$	$(10{,}8 \times 10^{-6} m^3)$
C_c:	Coupler compliance of Type 4220	$1{,}3 \times 10^{-10} m^5/N$	$(18{,}4 \times 10^{-6} m^3)$
C_d:	Compliance of dummy mic. cavity	$1{,}76 \times 10^{-12} m^5/N$	$(2{,}5 \times 10^{-7} m^3)$
C_m:	Compliance of loading mic. cavity	$1{,}76 \times 10^{-12} m^5/N$	$(2{,}5 \times 10^{-7} m^3)$
L_c:	Acoustical mass of the coupling element	$200\ kg/m^4$	
R_c:	Acoustical resistance of the coupling element	$1{,}82 \times 10^6\ Ns/m^5$	
	Source: Pistons of Type 4220	$\omega \times 4{,}42 \times 10^{-9} m^3/s$	$(\omega = 2\pi \times 250\ Hz)$

87

Fig. 2. Model of the calibrator driven by the pistonphone with values valid at 1013 ml and 20°C. The microphones are placed in the ports (1) and (3) for intensity or veloc calibration

phone, B & K Type 4220 was chosen for operations of this mode. See model of the calibrator in Fig. 2.

The magnitude and phase differences between the pressure of the ca ties, (b)–(a) have been measured and calculated, see Fig. 3 which al shows that within the range from a few Hz to about 500 Hz the phase d ference between the ports is nearly equal to the free-field phase lag f points 50 mm apart. When driven by a pistonphone at 250 Hz the sou

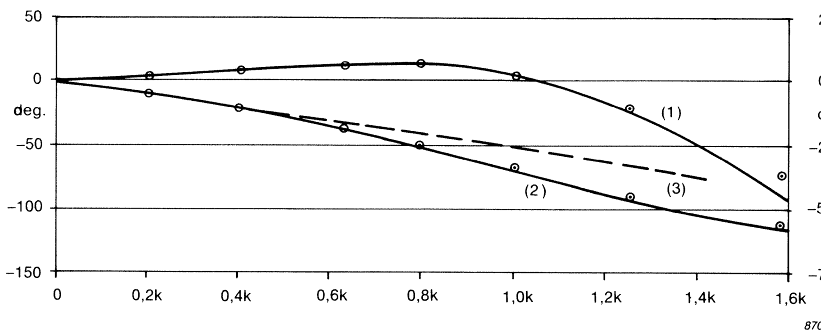

87

Fig. 3 Magnitude difference (1) and phase difference (2) between the pressure of t calibrator cavities, (b)–(a) were measured (curves) and calculated (points). The dott line (3) shows the free-field phase lag for points 50 mm apart at 20°C ssure levels of the cavities are nominally 118 dB therefore the particle ocity and intensity levels are also close to this value.

)ue to the phase linearity with frequency the levels are not critical with pect to frequency. At 250 Hz the slopes are as small as + 0,7 × 10^{-3} dB/ for intensity and + 1,5 × 10^{-3} dB/Hz for velocity.

ıvironmental Influences

e pressure and intensity levels as functions of the ambient pressure re measured with an FFT-analyzer and together with the particle veloc- level they were also calculated by use of the model. The results are ;ed in the table below.

\ttention should be paid to the agreement between the measured and calculated results and to the fact that the intensity level is practically lependent of the ambient pressure. Notice that the pressure level follows ambient pressure (last line of the table) while the particle velocity level ›ws the same changes but in the opposite direction.

3y measurement and calculation the temperature coefficient of the in- ısity level has been found to be + 0,024 dB/°C.

mb. pressure, p_a	mbar	700	800	900	994	1000	1013
measured	dB	−0,12	−0,07	−0,02	0	+0,01	−
calculated	dB	−0,06	−0,03	−0,01	0	0	0
cav.(a) measured	dB	−2,89	−1,80	−0,82	0	+0,05	−
cav.(a) calculated	dB	−2,87	−1,79	−0,82	0	+0,05	+0,16
calculated	dB	+2,93	+1,82	+0,83	0	−0,05	−0,15
) log (p_a/994)	dB	−3,05	−1,89	−0,86	0	+0,05	+0,16

T01649GB0

otes for Application of the Calibrator

ıe calibrator is designed for laboratory as well as field use. The calibrator pplies sound pressure to the microphone diaphragms only. The calibra- r works correctly with the newly introduced microphone types which are pecially designed for intensity measurements and which have extremely w vent-sensitivity.

In the calibration mode for intensity sensitivity only very small errors ll occur with ordinary measurement microphones while significant er- rs might occur in the mode for measurement of residual intensity index, pecially at low frequencies.

Accuracy and Calibration of the Intensity Calibratc

Determination of the calibrator's intensity and particle velocity levels quires calibration of sound pressure, frequency and of the phase differer between the cavities which is more simple to measure than might be (pected as microphones with known phase characteristics are not needt

Calibration can be made with any two microphones which load the cc pler correctly, i.e. with 250 mm^3. During the first phase measurement t microphones are inserted arbitrarily in the ports (1) and (3) while they ε interchanged before the second measurement. The difference between t results is twice the phase difference between the cavities. The meth eliminates a possible phase difference between the channels of the appli phase meter. The resulting calibration levels are found by inserting t measured values in the formulae given under the discussion of the me surement principle.

An accuracy of the intensity calibration level better than 0,15 dB is rat er easy to obtain and seems relevant in practice as artificial stability te: have given very promising results for the calibrator.

Conclusion

An intensity calibrator with a possible accuracy of 0,1 dB has been dev oped. The calibrator can simulate two angles of sound incidence on t intensity probe, 0° or 90°. In the 0°-mode sensitivity of measurement sy tems can be calibrated while in the 90°-mode the residual intensity ind can be measured.

It might be necessary to correct the calibrator's intensity level for t temperature but the ambient pressure has practically no influence at a

The principle is new but the properties of the calibrator have been me sured under different environmental conditions and a model has be worked out. The good agreement between the behaviour of the calibrat and the model shows that all significant physical effects are known.

For assistance with the experiments the author wishes to thank Halfdaner.

References

[1] Rasmussen, G., Brock, M. — *"Transducers for intensity measurements"*, IC Paris '83

[2] Frederiksen E. — *"Pressure microphones for intensity measuremen with significantly improved phase properties"*, IC Toronto, '86

reviously issued numbers of rüel & Kjær Technical Review

ontinued from cover page 2)

1982 Sound Intensity (Part II Instrumentation and Applications)
Flutter Compensation of Tape Recorded Signals for Narrow Band Analysis
1982 Sound Intensity (Part I Theory).
1982 Thermal Comfort.
1982 Human Body Vibration Exposure and its Measurement.
1981 Low Frequency Calibration of Acoustical Measurement Systems.
Calibration and Standards. Vibration and Shock Measurements.
1981 Cepstrum Analysis.
1981 Acoustic Emission Source Location in Theory and in Practice.
1981 The Fundamentals of Industrial Balancing Machines and Their Applications.
1980 Selection and Use of Microphones for Engine and Aircraft Noise Measurements.
1980 Power Based Measurements of Sound Insulation.
Acoustical Measurement of Auditory Tube Opening.
1980 Zoom-FFT.
1980 Luminance Contrast Measurement.
1979 Prepolarized Condenser Microphones for Measurement Purposes.
Impulse Analysis using a Real-Time Digital Filter Analyzer.
1979 The Rationale of Dynamic Balancing by Vibration Measurements.
Interfacing Level Recorder Type 2306 to a Digital Computer.
1979 Acoustic Emission.

pecial technical literature

rüel & Kjær publishes a variety of technical literature which can be obtained om your local Brüel & Kjær representative.
he following literature is presently available:

- Mechanical Vibration and Shock Measurements (English), 2nd edition
- Modal Analysis of Large Structures–Multiple Exciter Systems (English)
- Acoustic Noise Measurements (English), 3rd edition
- Architectural Acoustics (English)
- Noise Control (English, French)
- Frequency Analysis (English)
- Electroacoustic Measurements (English, German, French, Spanish)
- Catalogues (several languages)
- Product Data Sheets (English, German, French, Russian)

ırthermore, back copies of the Technical Review can be supplied as shown in ıe list above. Older issues may be obtained provided they are still in stock.

Brüel & Kjær

DK-2850 Nærum · Denmark · Telephone: +45 2 80 05 00 · Telex: 37316 bruka dk · Fax.: 02 80 14(

ISSN 007–2621